Optical Materials 32 (2010) 1337–1340

Contents lists available at ScienceDirect

Optical Materials

journal homepage: www.elsevier.com/locate/optmat

Scintillation mechanism of Tb^{3+} doped BaY_2F_8

Ana C.S. de Mello [a,*], Adriano B. Andrade [a], Gerson H.G. Nakamura [b], Sonia L. Baldochi [b], Mário E.G. Valerio [a]

[a] Physics Departament, Federal University of Sergipe, 49, 100-000 São Cristovão, SE, Brazil
[b] IPEN-CNEN/SP, CP 11049, 05422-970 São Paulo, SP, Brazil

ARTICLE INFO

Article history:
Received 4 November 2009
Received in revised form 14 April 2010
Accepted 22 April 2010
Available online 9 June 2010

Keywords:
BaY_2F_8
Tb^{3+} doping
Scintillator
TL emission
Radiation damage

ABSTRACT

In the present work, we report the optical properties of BaY_2F_8 doped with different concentrations of Tb^{3+} ions and its potential use as a scintillator in radiation detection. Two types of samples were studied: polycrystalline samples obtained via solid state reaction, and single crystals obtained via the zone melting method under a HF flow. The scintillating properties Tb^{3+} doped BaYF were checked by measuring the radioluminescence when excited with X-ray, showing intense emission peaks characteristics of rare-earth ion. Thermoluminescence measurements were done to study the traps competing to inhibit the scintillating process. The radiation damage was evaluated and it was shown that the formation of the absorption bands can be connected to color centers generated by radiation in the matrix. Measurements of DXAS revealed that there is no change in the absorption edge of the dopant during irradiation revealing that the color centers are not connected to changes in the valence of the dopants.

1. Introduction

Barium yttrium fluoride (BaY_2F_8 – BaYF) doped with trivalent rare-earth ions are promising materials for solid-state optical devices. In this paper, Tb-doped BaYF samples with different concentrations were studied aiming the use of scintillation devices in radiation detection. Scintillators have a wide variety of applications in medicine, industries and high energy physics [1].

The crystal structure of BaYF is monoclinic, and the trivalent rare-earth dopant ions are expected to occupy the Y^{3+} site [2]. The Y^{3+} sites show 8-fold coordination to 8 F^- ions having a C_2 point symmetry [3]. Recently BaYF doped rare-earth ions gained attention due to possible applications as a scintillator [3] and a laser host [4,5]. Rare earth doped BaYF may be used as scintillators due to their high light output and also the useful wavelength emission that can be tuned by choosing the right rare earth dopant that matches the light detection device [6]. The objective of this paper is to understand the dependency between the scintillator properties as a function of doping concentration and understand the radiation damage generated in the samples after irradiation.

The scintillation mechanism was studied via a combination of thermoluminescence (TL), radioluminescence (RL), optical absorption (OA) and dispersive X-ray absorption spectroscopy (DXAS) measurements in samples with different concentration of dopants. The combination of TL and RL is useful to study the trapping centers and to identify the ones related to the scintillation mechanism. Radiation damage studied via OA techniques can reveal the formation of the color centers generated by radiation in the matrix. DXAS was done simultaneously with RL measurements to study the relation between the darkening of the sample due to the color centers and the possible involvement of the Tb ions in such defects.

2. Methodology

The polycrystalline samples of RE-doped BaYF were prepared in a platinum reactor from stoichiometric mixture of BaF_2 and YF_3. Tb are added in concentrations of 0.5, 1.0, 2.0 and 3.0 mol%. The starting materials were melted at 960 °C under a HF flow in Pt crucibles. The single crystals were prepared from the synthesized powders by the floating zone melting method, under a HF atmosphere, in the concentrations of 2.0 and 3.0 mol% of Tb. Powder samples were prepared by grinding the obtained materials in agate mortar.

The structural analyses of the polycrystalline and single crystals powders samples were done via XRD measurements, performed at room temperature in a Rigaku DMAX Ultima+ 2000/PC diffractometer in the 2θ range from 13° to 80° in step scan mode, with steps of 0.02°, using Cu Kα radiation. RL spectra were recorded exciting the samples with Cu Kα X-rays (40 kV/40 mA) at room temperature. The spectra were collected using an optical fiber attached to an Ocean Optics HR2000 spectrometer. The scintillation efficient or light output for each sample can be obtained from the integration of its RL spectrum. A CsI:Tl sample was used as a standard sample and the scintillation efficiencies of all samples were obtained using the CsI:Tl light yield as reference.

* Corresponding author. Address: Departamento de Física, Universidade Federal de Sergipe, 49100-000 – São Cristóvão, SE, Brazil. Tel.: +55 79 21056636; fax: +55 79 21056807.
E-mail address: acarol_mello@yahoo.com.br (A.C.S. de Mello).

0925-3467/$ - see front matter © 2010 Elsevier B.V. All rights reserved.
doi:10.1016/j.optmat.2010.04.016

The TL measurements were done from room temperature up to 400 °C following a linear heating program with a heating rate of 5 °C/s, in a homemade TL reader. The samples were irradiated with X-rays with rate dose of 0.0924 Gy.

The OA spectra were obtained via diffuse reflectance using a polychromatic light source (Mikropack DH-2000 UV–Vis–NIR) and an optical fiber attached to Ocean Optics HR2000 spectrometer. DXAS measurements were done at the Brazilian Synchrotron Light Laboratory (LNLS) in the DXAS beamline at room temperature. Polychromatic X-ray beam is tuned close to the energy of the L_3 edge of Tb ions in a way that a full EXAFS or XANES spectrum is recorded in one shot in about 100 ms. The spectra were recorded as a function of the irradiation time in order to check if there is any change in the absorption edge of the dopant. At the same time, the RL was recorded, and in this way, any changes in the emission spectra can also be followed while the sample is irradiated.

3. Results and discussion

Fig. 1 presents the XRD powder patterns of the polycrystalline samples and the single crystals with different concentrations of Tb^{3+}. It can be observed that in all samples the predominant phase BaY_2F_8 is presented. In the polycrystalline 2.0 mol% doped samples a small amount of the phase $Ba_4Y_3F_{17}$ can be present but this undesirable phase can be eliminated after crystallization. In the 2.0 mol% doped single crystals only the BaY_2F_8 phase was detected. This is a clear indication that floating zone melting method is efficient in eliminating the phase $Ba_4Y_3F_{17}$.

The scintillator properties of Tb^{3+} doped BaYF powder can be seen in Fig. 2. This figure shows the RL spectra of different concentrations BaYF:Tb^{3+} samples excited by X-rays as compared to the commercial CsI:Tl scintillator material. The RL measurements of the BaYF:Tb^{3+} showed emission peaks in energies that are characteristics of the 4f–4f transitions of the trivalent rare earth ions [6]. The Tb^{3+} doped samples exhibit an RL spectrum with a maximum emission around 545 nm due to the $^5D_4 \rightarrow {}^7F_5$ transitions, corresponding to the green region of the visible spectrum. The single crystal samples with 3.0 mol% Tb^{3+} exhibited a quite intense emission, while the polycrystalline samples doped with 0.5 mol% Tb^{3+} showed the weakest emission intensity. The samples doped with 2.0 or 3.0 mol% Tb either polycrystalline or single crystals, showed RL intensity at 545 nm two times higher than CsI:Tl. This is the spectral region where the photomultiplier tubes are normally more efficient, pointing out a possible use of this material in scintillator devices.

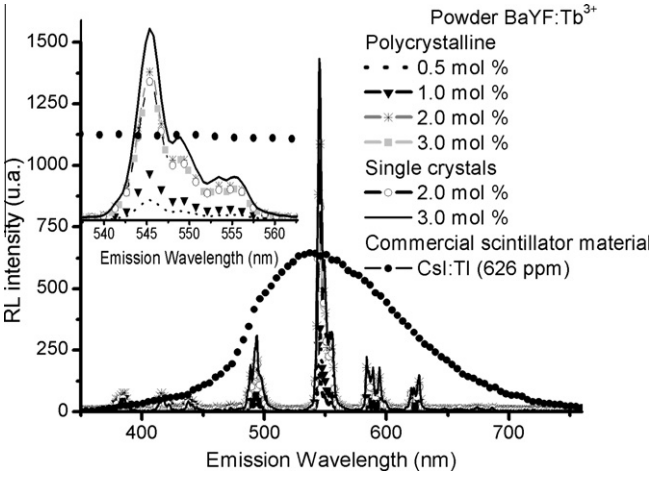

Fig. 2. RL spectra of the Tb-doped BaYF single crystals and polycrystalline samples with different concentrations of Tb and irradiated with X-rays. The inset shows the expanded region of the main RL emission peaks associated to the $^5D_4 \rightarrow {}^7F_5$ transitions of the Tb^{3+} ions.

The light output of each scintillator can be obtained from the integration of the RL spectrum. Table 1 presents, in the second column, the scintillation efficient for each sample normalized to the total emission of the CsI:Tl samples. The total RL efficiency of all BaYF:Tb^{3+} samples are lower than CsI:Tl scintillator that has a broad emission spectrum. Nevertheless the light yield from BaYF:Tb^{3+} samples are enough since some of the most commonly used scintillators like BGO ($Bi_4Ge_3O_{12}$) shows just 21% of the light yield of the CsI:Tl [1,9] and it is still used in many applications. The 2.0 and 3.0 mol% Tb^{3+} doped samples showed scintillation efficient of approximately three times greater than the other doped samples. The polycrystalline sample doped with 2.0 mol% Tb^{3+} presents higher scintillation efficiency than the single crystal doped with the same amount of Tb and this effect is not clear yet but it might be connected to the presence of the $Ba_4Y_3F_{17}$ phase in the polycrystalline samples. On the other hand, the single crystal samples

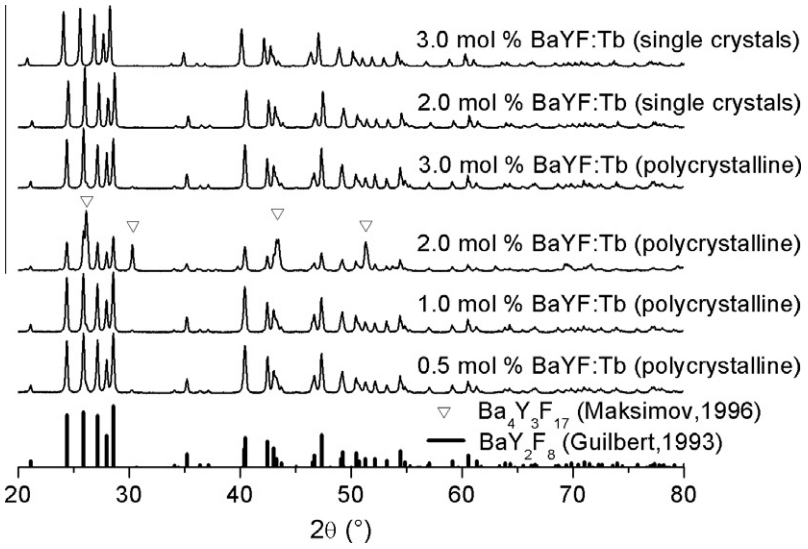

Fig. 1. XRD powder pattern of the single crystals and polycrystalline samples of BYF:Tb^{3+}. All diffraction peaks were identified to either the BaY_2F_8 [7] or BaY_4F_{17} [8] standard patterns.

Table 1
Scintillation efficient of the BaYF:Tb^{3+} single crystals and polycrystalline samples compared with CsI:Tl scintillator material and density of trapping compared with scintillation efficient of the Tb-doped BaYF.

Sample	Scintillation efficient (normalized to CsI:Tl)/%	Scintillation efficient (normalized to the BaYF:3 mol% Tb^{3+})/%	Density of trapping/ %
0.5 mol% (polycrystalline)	3.3	18.3	70.3
1.0 mol% (polycrystalline)	6.2	34.2	77.4
2.0 mol% (polycrystalline)	13.3	73.8	27.2
3.0 mol% (polycrystalline)	15.6	86.2	100.0
2.0 mol% (single crystals)	12.9	71.2	31.4
3.0 mol% (single crystals)	18.1	100.0	23.0
CsI:Tl (626 ppm)	100.0		

doped with 3.0 mol% has a higher intensity among all samples, including the polycrystalline one doped with the same amount of Tb.

Fig. 3 gives the TL curve of the pure and doped BaYF samples. The glow curve of the pure single crystals shows only 1 peak at 123 °C while the Tb^{3+} doped polycrystalline shows 2 extra peaks at 250 °C and a shoulder at about 350 °C. The only exception is the 2.0 mol% Tb^{3+} which shows only a shoulder at 180 °C. The reduction of the second peak could be due to the presence of $Ba_4Y_3F_{17}$ phase in this sample.

The density of traps associated to the overall TL emission can be estimated from the area under the glow curves. The area under the curves of Fig. 3 was normalized to the highest TL emission curve obtained for the 3.0 mol% doped BaYF polycrystalline samples. In Table 1 the areas are shown in the fourth column. There is a clear trend indicating that the higher the density of TL traps the lower the scintillation efficiency. This implies that these TL peak traps are competing to inhibit the scintillating process. The only exception for this behavior is the 3.0 mol% doped polycrystalline samples.

All the samples presented radiation damage and this refers to the change of scintillation efficiency due to defect creation by the radiation dose [10]. Fig. 4 shows RL intensity of emission peak at 545 nm ($^5D_4 \rightarrow {}^7F_5$) firstly increasing up to 0.49 Gy and then decreasing as a function with the absorbed dose indicating the buildup of radiation damage. Darkening of Tb-doped BaYF samples are observed after irradiation for all samples.

The radiation damage was evaluated by the optical absorption obtained from the reflectance spectra of the irradiated regions in the powdered samples. The results are shown in Fig. 5 for the pure and the doped samples irradiated with a dose of 0.462 Gy of X-rays. Three main absorptions bands are observed in all samples with maximum approximately at 289, 468 and 603 nm. The single crystal doped with 3.0 mol% of Tb showed an extra band at about 812 nm. These results showed that the position of the absorption bands due to the radiation induced color centers are independent of doping, although the relative intensities of this OA bands may vary according to the doping level. This is a strong indication that the defects centers generated by irradiation are directly linked to the BaYF matrix. The most probable defects in fluorides are F-type centers (F, F^- or F_A centers) and modified V_k centers that are known to produce absorption bands in the 300–330 nm, 240–380 nm, and 450–600 nm regions in other fluoride matrixes [11,12].

Fig. 6 shows the X-ray absorption edge of the Tb ions for the 2.0 mol% doped single crystals as compared to the absorption

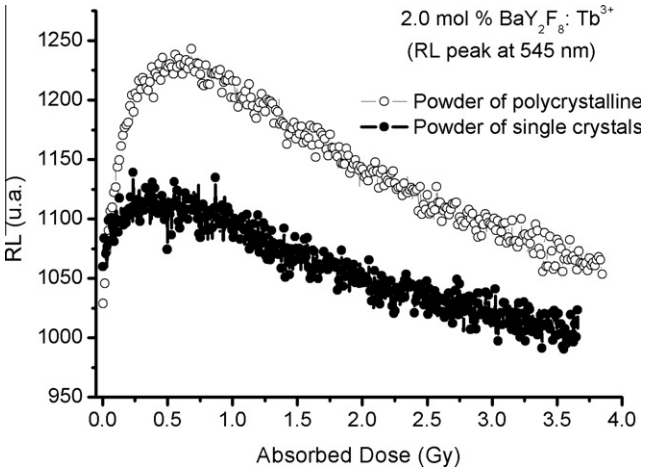

Fig. 4. RL intensity of the emission peak at 545 nm as a function with absorbed dose of the X-rays.

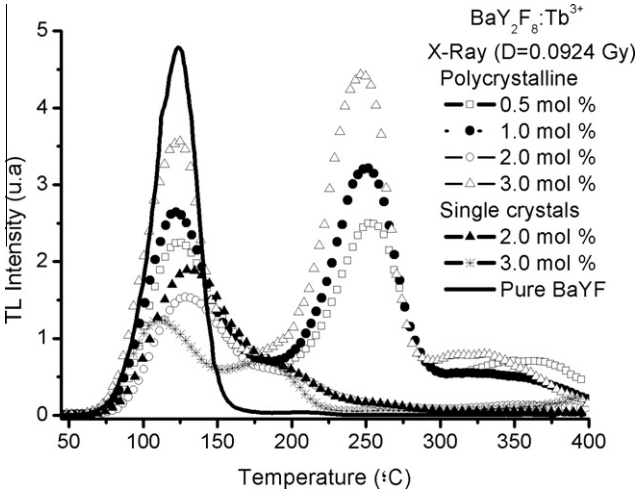

Fig. 3. Thermoluminescence glow curves of pure single crystals, doped BaYF:Tb^{3+} single crystals and polycrystalline doped samples with different concentrations of Tb and irradiated with 0.0924 Gy of X-rays.

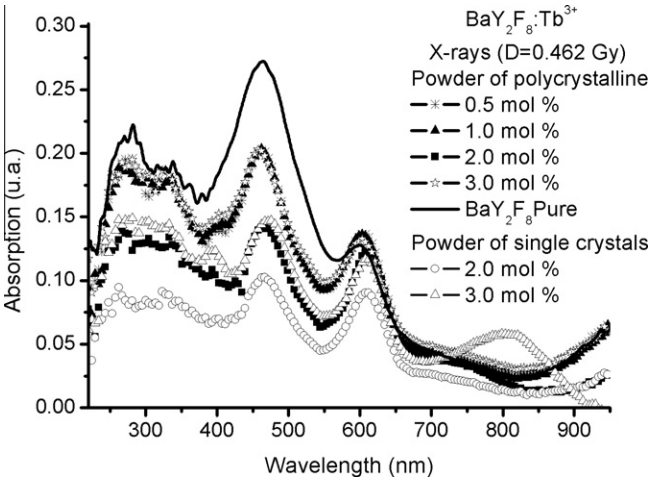

Fig. 5. OA spectra of pure and Tb-doped BaYF single crystals and polycrystalline samples irradiated with 0.462 Gy of X-rays.

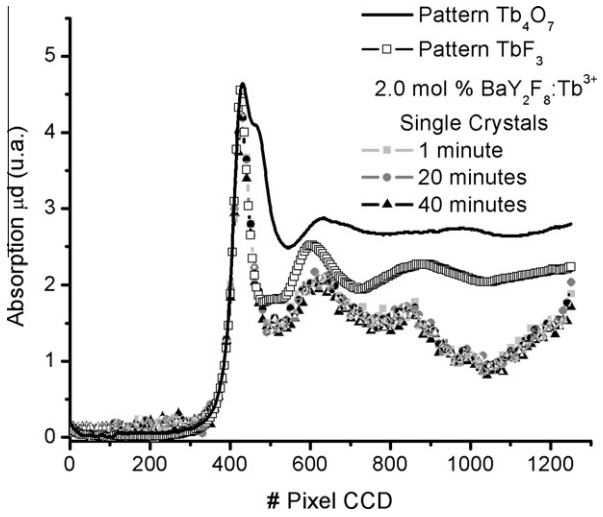

Fig. 6. Comparison of the XANES measurements near to the absorption edge of Tb^{3+} ions in BaYF sample compared to the XANES of TbF_3 and Tb_4O_7 standard materials. The measurements were done using the DXAS beamline at the LNLS. The horizontal axis indicates the pixel in the CCD camera that is directly proportional to the energy of the incident X-rays. The absorption curves were not normalized and represent the raw data.

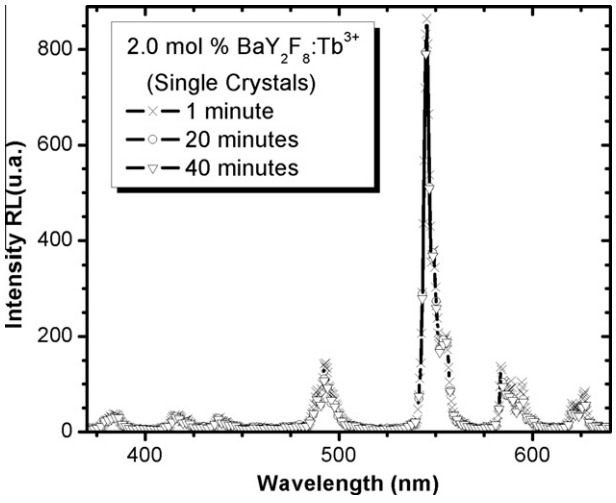

Fig. 7. RL spectra of the 2 mol% Tb-doped BaYF single crystals samples irradiated with synchrotron light at three irradiation times obtained simultaneously with DXAS measurements.

edges of the Tb ions in two standard compounds TbF_3 and Tb_4O_7. In the first one, Tb is found only in the trivalent state, while in the second one, there is a mixture of the Tb^{3+} and Tb^{4+} charge states. It can be seen that the absorption edge of the Tb-doped BaYF samples is very close to the Tb found in TbF_3 compounds and that there is no change in the absorption edge during the whole period of irradiation. The three measurements taken after 1 min, 20 min or 40 min after starting the measurements did not show any significant change. The main difference of the TbF_3 standard pattern is the signal to noise ratio that is worse in the Tb-doped BaYF due to the small amount of Tb in the matrix as compared to the TbF_3 or Tb_4O_7 samples.

Radioluminescence (RL) measurements taken simultaneously with DXAS measurements are shown in Fig. 7. Again the results show that there is no change in the positions of the RL peaks during irradiation, only a change in RL intensity due to radiation damage. The DXAS results combined with the simultaneous measurements of the RL indicate clearly that there is no direct participation of the Tb ions in the buildup of the radiation damage, since no evidence of valence change or change in the emission spectra were found during irradiation, and this supports the OA results that the main source of the radiation damage must come from the BaY_2F_8 matrix.

4. Conclusions

This work presents new evidences to understand the scintillating properties of Tb-doped BaY_2F_8 samples revealing some important aspects of the interaction of the ionizing radiation with the material and some aspects of the mechanism of the light emission. It was shown that single crystals and polycrystalline samples doped with 2.0 or 3.0 mol% of Tb^{3+} are promising solid-state systems for radiation detection and possible applications may be devised in scintillators due to their relatively intense light yield and also the useful wavelength emission. TL results indicate that the presence of a range of competing charge traps that can decrease the RL. On the other hand, it also showed that the higher concentrated samples have less concentration of traps. All the samples presented radiation damage revealed by the formation of the absorption bands that can be connected to color centers generated during radiation. This radiation damage influences the RL intensity, a combination of dispersive X-ray absorption measurements with simultaneous RL measurements, which revealed that the Tb dopant did not participate directly in the formation of the color centers induced by the radiation. And this is an indication that these color centers are connected to the defects in the BaYF matrix.

Acknowledgements

The authors gratefully acknowledge the CNEN, CAPES, CNPq, and FAPESP for financial support. The authors also acknowledge the LNLS (Brazilian Synchrotron Light Laboratory) for the support and the use of the DXAS and XAFS beamlines (Projects XAFS 6743 and 7285, and DXAS 6754, 6707 and 7311).

References

[1] G. Blasse, Chem. Mater. 6 (1994) 1465.
[2] J.B. Amaral, M.A.C. Santos, M.E.G. Valerio, R.A. Jackson, Appl. Phys. 81 (2005) 841.
[3] J.C. van't Spijker et al., J. Lumin. 85 (1999) 11.
[4] F. Cornacchia, D. Parisi, C. Bernardini, A. Toncelli, M. Tonelli, Opt. Express 12 (2004) 1982.
[5] A. Agnesi et al., Opt. Express 12 (2004) 3765.
[6] M.E.G. Valerio, V.G. Ribeiro, A.C.S. Mello, M.A.C. Santos, S.L. Baldochi, V.L. Mazzocchi, C.B.R. Parente, R.A. Jackson, J.B. Amaral, Opt. Mater. 30 (2007) 184.
[7] L.H. Guilbert, J.Y. Gesland, A. Bulou, R. Retoux, Mat. Res. Bull. 28 (1993) 923.
[8] B.A. Maksimov, H. Solans, A.P. Dudka, E.A. Genkina, I.I. Buchinskaya, A.A. Loshmanov, A.M. Golubev, V.I. Simonov, J. Kristal. 41 (1996) 51.
[9] G.F. Knoll, Radiation Detection and Measurement, Wiley, New York, 1989. pp. 215–240.
[10] C. Greskovich, S. Duclos, Ann. Rev. Mater. Sci. 27 (1997) 69.
[11] M.K. Sławomir, B. Amina, B. Georges, Opt. Mater. 28 (2006) 123.
[12] G.M. Marolo, G. Baldachini, V.S. Kalinov, E.R.M. Monterealli, Phys. Stat. (c) 2 (2005) 367.